IX CONGRESSO BRASILEIRO DE ENGENHARIA E CIÊNCIAS TÉRMICAS
9th BRAZILIAN CONGRESS OF THERMAL ENGINEERING AND SCIENCES

Paper CIT02-0425

COMPUTATIONAL SIMULATIONS OF THE CREAM INJECTION DURING THE PROCESS OF MILK STANDARDIZATION

Flávia Schwarz Franceschini[1]
Laboratory of Applied and Computational Fluid Mechanics (LAMAC)
Universidade Federal do Rio Grande do Sul (UFRGS)
Rua Sarmento Leite nº 425. CEP: 90050-170. Porto Alegre – RS, Brazil
fla@mecanica.ufrgs.br

Daniel H. Girotti-Fontana[2]
Laboratory of Applied and Computational Fluid Mechanics (LAMAC)
Universidade Federal do Rio Grande do Sul (UFRGS)
Rua Sarmento Leite nº 425. CEP: 90050-170. Porto Alegre – RS, Brazil
dgirotti@mecanica.ufrgs.br

Sérgio Frey[3]
Laboratory of Applied and Computational Fluid Mechanics (LAMAC)
Universidade Federal do Rio Grande do Sul (UFRGS)
Rua Sarmento Leite nº 425. CEP: 90050-170. Porto Alegre – RS, Brazil
frey@mecanica.ufrgs.br

Abstract. *The main goal of this study is to simulate the cream injection in skimmilk, which occurs in the process of milk standardization, visualizing the mass transfer along the process line. The problem was approximated by the finite element method. To perform some 2D simulation, the velocity field obtained using a commercial code was given as input to the code developed for this research, to solve the mass fraction field. For a more realistic simulation, a 3D mesh was implemented using a commercial code. The method employed to reach numerical stabilization was Streamline Upwind/Petrov-Galerkin (SUPG). The results using SUPG were compared to those using classical Galerkin approximation. The SUPG method shows a good feature of smoothing numerical instabilities.*

Keywords*. Continuum Mechanics, SUPG, Food Processing*

1. Preliminaries

Problems in Food Engineering have been solved much using experimental techniques, due to the food industry has still a strong basis on empiricism and a lack of Engineering research, specially in economically emerging countries. Even though, Computational Fluid Dynamics (CFD) also finds a great application in this area. It makes possible to predict the behavior of foods during their process without a great expense of money or raw materials (Kumar & Swartzel, 1993; Xia & Sun, 2002).

The process of milk standardization consists on the controlled injection of cream with a high percentage of fat in skimmilk, in order to obtain a final product with standard fat content. In modern milk processing plants, direct in-line standardization is commonly used. In dairy industries, this process occurs right after milk centrifugation, where the high percentage fat part, the milk cream, is separated from the low fat part, the skimmilk. The proportions to get a final fat content are calculated by the control system before the cream is re-injected into the skimmilk. Changes in flow rates through the centrifugal separator and variations of the incoming whole milk fat content are compensated by an accurate density control combined with constant pressure control at the skimmilk outlet on the separator, ensuring the necessary conditions for the remixing (TetraPak, 1995)

[1] This author is a graduate student at the Mechanical Engineering Program (PROMEC)/UFRGS.
[2] This author is an undergraduate student at Mechanical Engineering Department/UFRGS.
[3] All correspondence should be mailed to this author

In this paper a mechanical model of the injection of cream in skimmilk is proposed. Some results of solving the mechanical model are of engineering importance. One is the velocity field along the flow, indicating velocity profiles that are responsible for the convection of one component into another. Other is the pressure field, giving the pressure drop, an important Engineering parameter. The mass fraction field calculated along the flow gives a good idea of how the cream is convected into skimmilk in this process.

The main goal of this paper is to simulate this phenomena using a finite element approximation. In a first step, a 2D geometry was employed. To solve the velocity field, the equations of mass and momentum balance were solved for a bulk fluid, with constant properties along the domain. The velocity field was used as an input for the program developed to solve the local mass concentrations, using the species mass balance equation. As the problem is strongly convective, some numerical instabilities are generated by the classical Galerkin approximation, creating the need for a stabilization method. The stabilized method used then was the Streamline Upwind/Petrov-Galerkin (SUPG) (Brooks & Hughes, 1982). Some results are given and compared to the classical Galerkin approximation results.

In order to obtain more realistic results, with industrial interest, simulations employing a 3D geometry were performed. The analysis consisted in comparing four different diameters for the cream pipe, evaluating the mass transfer effectiveness in completing the mixture. All 3D simulations were performed using a commercial code.

Figure (1) is a representation of the problem statement.

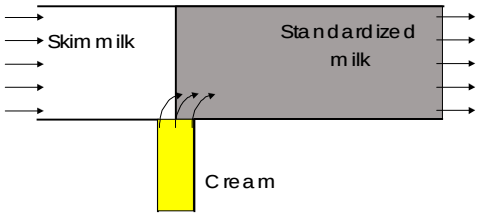

Figure 1:Problem statement

1.1 Mass balance in the control system

In modern milk processing plants, direct in-line standardization is usually combined with separation. Control valves, flow and density meters and a computerized control loop are used to adjust the fat content of milk and cream to desired values. This system controls the amount of cream injected in the skimmilk, which depends on their fat levels after separation. This amount is calculated as follows.

Let X_m be the desired fat percentage in the standardized milk. Let X_c and X_s be the fat percentage of cream and skimmilk after separation, and F_c, F_s and F_m the momentaneous flows of each component cream, skimmilk and standardized milk. A mass balance over the problem's domain represented in Fig. (1) gives:

$$\begin{aligned} F_c X_c + F_s X_s &= F_m X_m \\ F_c + F_s &= F_m \end{aligned} \tag{1}$$

As the quantities X_c and X_s are measured by an in-line density meter, Eqs. (1) give enough information to the controller to set the amount of cream to be injected.

The Reynolds number is determined based on the mean velocity of the whole mixture, considered the bulk fluid:

$$\mathrm{Re} = \frac{D_h \bar{U} \rho}{\mu} \tag{2}$$

in which A is the pipe's cross section and ρ and μ are the density and the viscosity of the mixture.

The bulk fluid physical properties should be evaluated as a pondered average of the fluids flowing in the considered region. As the mass fractions are not known before solving the problem, these properties are estimated based on a pondered average of the desired final concentrations. This is possible also because the two fluids have very similar properties. It is important to have a good estimate of the Reynolds number before performing any numerical or practical experiment, because if the flow is not laminar (for Re>2000), some different aspects regarding turbulence should be taken into account.

2. Mechanical modeling

To model the problem, some concepts of Continuum Mechanics (Slattery, 1999) are used. Also, some hypothesis are taken to simplify the problem to one more adapted to the main goal of this research.

The most common hypothesis applied here are: steady state, incompressible flow, bulk newtonian fluid, 2D domain, constant physical properties. The bulk fluid hypothesis is the same as to consider the mixture as a dilution of one component into another, with out changing its properties. This hypothesis is applied to calculate the velocity field

through the momentum and mass balance equations. The velocity field is imposed to the species mass transfer problem, uncoupling the problems of velocity-pressure and mass conduction-convection.

2.1. Mass balance

The mass balance for the system is obtained employing Reynolds transport theorem (Truesdell & Toupin, 1960) for the density of the bulk fluid ρ. It results on the continuity equation (Slattery, 1999):

$$\frac{D\rho}{Dt} + \rho \,\mathrm{div}\,\mathbf{u} = 0 \tag{3}$$

where **u** is the velocity field and the operator $D(\cdot)/Dt$ denotes the material derivative (Slattery, 1999).

For incompressible materials, the motion is called isochoric (Slattery, 1999), and the continuity equation is given by div **u** = 0. This is the first of a system of equations to solve the velocity field to the injection problem.

2.2. Momentum balance

The momentum balance for a body is given by Euler's Firs Law (Truesdell & Toupin, 1960), expressed in the form:

$$\frac{d}{dt}\int_{Vm} \rho\mathbf{u}\,dV = \int_{Sm} \mathbf{t}\,dS + \int_{Vm} \rho\mathbf{f}\,dV \tag{4}$$

where **f** stands for the mutual forces field (negligible) and external forces field (gravitational field) for unit mass (Slattery, 1999), **t** is the stress per unit area vector, which represents the contact forces.

The stress tensor **T** is defined as $\mathbf{T}=T_{ij}\mathbf{e}_i\otimes\mathbf{e}_j$, in the tensorial basis $\mathbf{e}_i\otimes\mathbf{e}_j$, where each component T_{ij} is the ith-component of the stress vector acting upon the positive side of the plane x_j = constant (Slattery, 1999). In this way, Cauchy's theorem postulates that **t** = **T**·**n**, com **T** = $\mathbf{T}^T$. Substituting in Eq. (4), considering an incompressible fluid, rearranging and applying Green's transformation, and applying a localization argument (Gurtin, 1981), the remaining integrand of this equation equals to zero, resulting in the differential momentum balance, or Cauchy's First Law (Slattery, 1999):The momentum balance is then expressed as:

$$\rho\frac{D\mathbf{u}}{Dt} = \mathrm{div}\,\mathbf{T} + \rho\mathbf{f} \tag{5}$$

To model the tensor **T**, we consider the motions that cause stresses, that are the components of the symmetric part of the velocity gradient tensor ∇**u**, called rate of deformation tensor (**D**). The way that **D** affects **T** is the so called constitutive equation of the material. For a newtonian incompressible fluid (Truesdell & Noll, 1965), the constitutive equation is given by

$$\mathbf{T} = -p\mathbf{I} + 2\mu\mathbf{D} \tag{6}$$

The differential momentum balance, or Cauchy's First Law (Eq. (5)), is written as follows, with ν standing for the cinematic viscosity:

$$\frac{\partial\mathbf{u}}{\partial t} + (\nabla\mathbf{u})\mathbf{u} = -\frac{\nabla p}{\rho} + 2\nu\nabla\cdot\mathbf{D}(\mathbf{u}) + \mathbf{f} \tag{7}$$

2.3. Species mass balance

In a Continuum Mechanics context, a mixture of *n* species is imagined as a multicomponent body, wich is a sum of *n* single-component bodies with a variable density field. Instead of calculating fields such as velocity and pressure for each component in the mixture, the mechanical postulates are put in a multicomponent form. The equations to solve are then the same equations as for a single-component system, plus *n*–1 equations representing the mass balance for each species. The density and the mass-averaged velocity of a multicomponent system, and the mass fraction of a species in this system are given by:

$$\rho = \sum_{i=1}^{n}\rho_{(i)}; \quad \mathbf{u} = \frac{1}{\rho}\sum_{i=1}^{n}\rho_{(i)}\mathbf{u}_{(i)}; \quad \omega_{(i)} = \frac{\rho_{(i)}}{\rho} \tag{8}$$

The differential mass balance for each species is given, according to Slattery (1999), as:

$$\frac{\partial \rho_{(i)}}{\partial t} + \operatorname{div}\left(\rho_{(i)}\mathbf{u}_{(i)}\right) - r_{(i)} = 0 \tag{9}$$

where the species velocity $\mathbf{u}_{(i)}$ is defined together with the definition of the bulk velocity field $\mathbf{u}$, to give the mass flux of species i with respect to the bulk velocity as $\mathbf{j}_i = \rho_{(i)}\,(\mathbf{u}_{(i)} - \mathbf{u})$. Employing the definitions for $\mathbf{j}_i$ and $\omega_{(i)}$ in Eq. (9), it comes that

$$\rho \frac{D\omega_{(i)}}{Dt} + \operatorname{div}\mathbf{j}_{(i)} - r_{(i)} = 0 \tag{10}$$

The equation for the mass transfer rate for a binary mixture, or the Fick's Law, given by Eq. (10), makes it possible to formulate a simpler way of Eq. (10), Eq. (12), if it is considered that the density of the mixture is constant:

$$\mathbf{j}_{(i)} = \rho D_{ij} \nabla \omega_{(i)} \tag{11}$$

$$\frac{D\rho\omega_{(i)}}{Dt} + \operatorname{div}\left(\nabla \rho D_{ij}\omega_{(i)}\right) - r_{(i)} = 0 \tag{12}$$

where D_{ij} is the coefficient of binary diffusion of species i and j, which may vary with temperature and mass fractions, while ρ is always locally defined because of the variation of species mass fractions along the domain.

2.4. System of equations

The balances of the previous section, performed over the problem's domain $\Omega \in \mathbb{R}^2$, give the necessary equations to solve the velocity and pressure fields, so as the mass fraction field, if initial and boundary conditions (on the usual frontiers Γ_h and Γ_g), are also given. The bulk fluid is considered to be newtonian and no mass generation exists. Using the previous hypothesis, a set of equations given below models the cream injection:

$$\begin{aligned}
&\frac{\partial \mathbf{u}^*}{\partial t^*} + \left(\nabla \mathbf{u}^*\right)\mathbf{u}^* + \nabla p^* - 2\,\mathrm{Re}^{-1} \operatorname{div}\mathbf{D}(\mathbf{u}^*) - \mathbf{f}^* = 0 \quad && \textit{over } \Omega \\
&\operatorname{div}\mathbf{u}^* = 0 && \textit{over } \Omega \\
&\frac{1}{\mathrm{St}}\frac{\partial \omega_{(i)}}{\partial t^*} + \nabla \omega_{(i)} \cdot \mathbf{u}^* - \frac{1}{\mathrm{Pe}_m}\operatorname{div}(\nabla \omega_{(i)}) = 0 && \textit{over } \Omega
\end{aligned} \tag{13}$$

where the non-dimensional variables are given by:

$$\mathbf{u}^* = \frac{\mathbf{u}}{\mathbf{u}_\infty}; \quad p^* = \frac{p}{\rho \mathbf{u}_\infty^2}; \quad \mathbf{f}^* = \frac{\mathbf{f}L}{\mathbf{u}_\infty^2}; \quad t^* = \frac{t\mathbf{u}_\infty}{L} \tag{14}$$

and the non-dimensional parameters that control the dynamic similarity of the flow are the Reynolds, Peclet and Schmidt numbers:

$$\begin{aligned}
&\mathrm{Re} = \frac{\mathbf{u}_\infty L}{\nu_0} \\
&\mathrm{Pe_m} = \mathrm{ScRe} = \frac{\mathbf{u}_0 L_0}{D_{ij}}; \\
&\mathrm{Sc} = \frac{\nu_0}{D_{ij}}.
\end{aligned} \tag{15}$$

The boundary conditions are: no-slippery condition at the walls; prescribed velocity $\mathbf{u}_g$ and prescribed mass fraction field $\omega_{(i)g}$ at the beginning of each pipeline; free-traction $\mathbf{T}_h$ and free mass-flux $j_{(i)h}$ at the outlet:

$$\begin{aligned}
&\mathbf{u}^* = \mathbf{u}_g^* && on\ \Gamma_g \\
&\omega_{(i)} = \omega_{(i)g} && on\ \Gamma_g \\
&\left[-p^*\mathbf{I} + 2\nu\mathbf{D}(\mathbf{u}^*)\right]\mathbf{n} = \mathbf{T}_h && on\ \Gamma_h \\
&\left[\rho D_{ij}\nabla\omega_{(i)}\right]\cdot\mathbf{n} = j_{(i)h} && on\ \Gamma_h
\end{aligned} \tag{16}$$

3. Finite element model

To the finite element modeling the finite subspaces $\mathbf{V}_h$, P_h (Franca & Frey, 1992) and W_h (Franca et al., 1992) are employed, defined as:

$$\mathbf{V}_h = \{\mathbf{v} \in H_0^1(\Omega)^N \,|\, \mathbf{v}_{|K} \in R_{|K}(K)^{nsd}, K \in \mathcal{C}_h\} \tag{17}$$

$$P_h = \{p \in \mathcal{C}_h^{\,0}(\Omega) \cap L_0^2(\Omega) \,|\, p_{|K} \in R_K(K), K \in \mathcal{C}_h\} \tag{18}$$

$$W_h = \left\{w \in H_0^1(0) \,|\, w_{|K} \in R_K(K), K \in \mathcal{C}_h\right\} \tag{19}$$

where $L^2(\Omega)$ defines the space of square integrable functions over Ω, $L_0{}^2(\Omega)$ the space of square integrable functions zero averaged over Ω, $H^1(\Omega)$ the Sobolev space of square integrable functions and first derivatives over Ω and $H_0{}^1(\Omega)$ the Sobolev space of square integrable functions and first derivatives over Ω that vanish on Γ_g.

The Galerkin approximation for the system gives the scheme:

Find the triple $(\mathbf{u}_h, p_h, \omega_{(i)h}) \in \mathbf{V}_h$, x P_h x W_h such as

$$B(\mathbf{u}_h, p_h, \omega_{(i)h}; \mathbf{v}, q, w) = F(\mathbf{v}, q, w), \quad (\mathbf{v}, q, w) \in \mathbf{V}^h \times P^h \times W^h \tag{20}$$

where

$$\begin{aligned}
B(\mathbf{u}_h, p_h, \omega_{(i)h}; \mathbf{v}, q, w) = &\left(\left[\nabla\mathbf{u}\right]\mathbf{u}, \mathbf{v}\right) + (2\nu\mathbf{D}(\mathbf{u}), \mathbf{D}(\mathbf{v})) - (\nabla\cdot\mathbf{v}, p) - (\nabla\cdot\mathbf{u}, q) \\
&+ \left([\nabla\omega_{(i)}]\mathbf{u}, w\right) + \left(D_{ij}\nabla\omega_{(i)}, \nabla w\right)
\end{aligned} \tag{21}$$

and

$$F(\mathbf{v}, q, w) = (\mathbf{f}, \mathbf{v}) + (\mathbf{T}_h, \mathbf{v})_{\Gamma_h} + \left(R_{(i)}, w\right) + (w, j_{(i)h})_{\Gamma_h} \tag{22}$$

3.1. Stabilization strategy

The numerical stability of advection-diffusion problems, such as the solution of the mass fraction field, is only possible when the problems related to the dominance are overcame. According to Hughes [5], the error of Galerkin approximation may be estimated as:

$$\left\|\phi - \phi^h\right\| \le C\,\mathrm{Pe}_h^m\, h^{k-1} \tag{23}$$

where ϕ and ϕ^h are the exact and numerical solutions for the scalar ϕ, respectively, h is the estimate of the element's ratio, C is a mesh independent constant, k is the degree of interpolation and $\mathrm{Pe}^m{}_h$ is the grid mass Peclet number, defines as:

$$\mathrm{Pe}_h^m = \frac{|\mathbf{a}|_p\, h}{2\mathsf{D}} \tag{24}$$

where $|\mathbf{a}|_p$ is the p norm (Euclidean for $p = 2$, infinite norm if $p = \infty$) of the advective field $\mathbf{a}$.

The grid Peclet is directly related to the approximation error. A high Peclet number, or $\mathrm{Pe}_h^m >> 1$, produces numerical oscillations that must be reduced even by refining the mesh or by the use of a stabilization scheme. The numerical difficulties associated to advection-diffusion problems have been overcome by different strategies like the Taylor-Galerkin, Characteristics-Galerkin (Brasil Junior et al., 1997), Streamline Upwind Petrov-Galerkin (Brooks & Hughes, 1982) and Galerkin Least Square (Hughes et al., 1988) methods.

In this paper, the stability given by a SUPG scheme is compared with results of classical Galerkin approximation. The SUPG scheme is based on the addition of artificial diffusion terms in the streamline direction. The weight function is modified to:

$$w_{SUPG} = w + \alpha[\nabla w]\mathbf{a} \tag{25}$$

where α are mesh dependent terms, which are multiplied by the residual of the Euler-Lagrange equations evaluated elementwise. As these residuals satisfy the exact solution, the Petrov-Galerkin scheme represents a consistent formulation.

The forms $B(\phi, w)$ and $F(w)$ are written, in the SUPG scheme, as follows:

$$\begin{aligned} B_{SUPG}(\phi, w) &= \left([\nabla\phi]\mathbf{a}, w\right) + \left(D\ \nabla\phi, \nabla w\right) \\ &+ \sum_{K\in C_h} \left([\nabla\phi]\mathbf{a} - D\ \Delta\phi, \alpha(\mathrm{Pe}_K^m)[\nabla w]\mathbf{a}\right)_K \end{aligned} \tag{26}$$

$$F_{SUPG}(w) = \left(R, w\right) + \left(j_h, w\right)_{\Gamma_h} + \sum_{K\in C_h} \left(R, \alpha(\mathrm{Pe}_K^m)[\nabla w]\mathbf{a}\right)_K \tag{27}$$

The α parameter is defined as in Franca et al. (1992), including the degree of interpolation in the definition of the grid Peclet number.

3.2. SUPG formulation

The complete SUPG formulation for the injection problem is then completed:
Find the triple ($\mathbf{u}_h$, p_h, $\omega_{(i)h}$)$\in$ $\mathbf{V}_h$, x P_h x W_h such as:

$$B(\mathbf{u}_h, p_h, \omega_{(i)h}; \mathbf{v}, q, w) = F(\mathbf{v}, q, w), \quad (\mathbf{v}, q, w) \in \mathbf{V}^h \times P^h \times W^h \tag{28}$$

where

$$\begin{aligned} B(\mathbf{u}_h, p_h, \omega_{(i)h}; \mathbf{v}, q, w) &= \left([\nabla\mathbf{u}]\mathbf{u}, \mathbf{v}\right) + (2\nu\mathbf{D}(\mathbf{u}), \mathbf{D}(\mathbf{v})) - (\nabla\cdot\mathbf{v}, p) - (\nabla\cdot\mathbf{u}, q) \\ &+ \left([\nabla\omega_{(i)}]\mathbf{u}, w\right) + \left(D_{ij}\nabla\omega_{(i)}, \nabla w\right) \\ &+ \sum_{K\in C_h} \left([\nabla\mathbf{u}]\mathbf{u} + \nabla p - 2\nu\nabla\cdot\mathbf{D}(\mathbf{u}), \tau(\mathrm{Re}_K)([\nabla\mathbf{v}]\mathbf{v} - \nabla q)\right)_K \\ &+ \sum_{K\in C_h} \left([\nabla\omega_{(i)}]\mathbf{u} - D_{ij}\Delta\omega_{(i)}, \alpha(\mathrm{Pe}_K^m)[\nabla w]\mathbf{u}\right)_K \end{aligned} \tag{29}$$

and

$$\begin{aligned} F(\mathbf{v}, q, w) &= (\mathbf{f}, \mathbf{v}) + (\mathbf{T}_h, \mathbf{v})_{\Gamma_h} + \left(R_{(i)}, w\right) + (j_{(i)h}, w)_{\Gamma_h} \\ &+ \sum_{K\in C_h} (\mathbf{f}, \tau(\mathrm{Re}_K)([\nabla\mathbf{v}]\mathbf{v} - \nabla q))_K + \sum_{K\in C_h} \left(R_{(i)}, \alpha(\mathrm{Pe}_K^m)[\nabla w]\mathbf{u}\right)_K \end{aligned} \tag{30}$$

The stability parameter for the velocity-pressure problem $\tau(\mathrm{Re}_K)$ depends on the grid Reynolds number Re_K and is defined as in Franca and Frey (1992).

4. Numerical results

The numerical simulations for obtaining the velocity field for the 2D model, and both velocity and mass fraction field for the 3D model were performed at the National Center of Supercomputation (CESUP), using a Silicon Graphics Octane Workstation dual processor with 128 Mb RAM. The software used was Flotran (ANSYS 5.7, Ansys Inc.). The simulations of the advection-diffusion problem for the 2D model were performed at the Laboratory of Applied and Computational Fluid Mechanics (LAMAC), using a Intel Pentium III with 1.1 GHz processor and 1 Gb RAM, using a program developed by the research group. The visual post processing was made with use of the software Ensight 7.

4.1. 2D simulations

A 2D geometry, using similar to industrial pipe measures, was used to implement the finite element solution.

The mesh created for the simulations consisted of 17540 Q_1 (bilinear quadrilateral) elements. The boundary conditions of velocity were such as to maintain a laminar regimen. Figure (2) shows the result for the velocity field that was input in the advection-diffusion program.

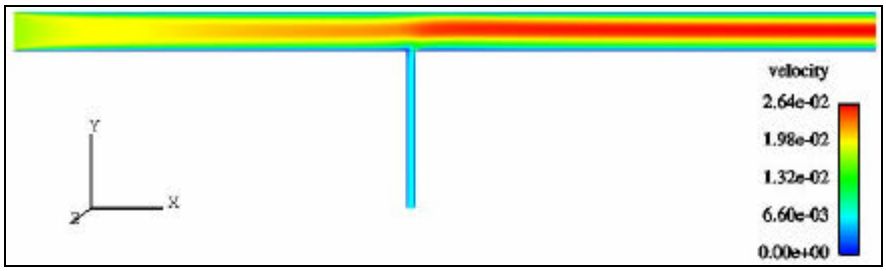

Figure 2: Velocity field

In each simulation, the value for the mass diffusivity was varied. The nodal values for velocity and the mesh were kept the same during all experiments. So the variation of the grid Peclet number was due to the mass diffusion coefficient.

The simulations covered the range $10^{-4} \leq Pe^m_K \leq 10^4$, performed using the classic Galerkin formulation, Eq. (20), and the SUPG formulation Eq. (28). The results are given as the mass fraction profile along the domain, shown in a detailed view.

Analyzing the result for $Pe^m_K = 10^{-4}$(Fig. (3)), it is verified that numerical instabilities are not produced. This is due to a very high mass diffusivity coefficient, which makes the problem diffusive dominated, and the advective field negligible. However, this value for the diffusivity is not physically realistic, and it is possible to observe dissolution of the components in a direction contrary to the flow.

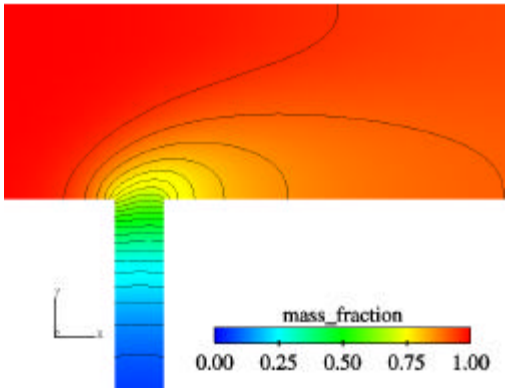

Figure 3: Result for $Pe^m_K = 10^{-4}$

For $Pe^m_K \leq 10^0$, instabilities were not verified. Figure 4 illustrates the quasi stable solution using Galerkin approximation for $Pe^m_K \approx 10^1$,showing light instabilities.

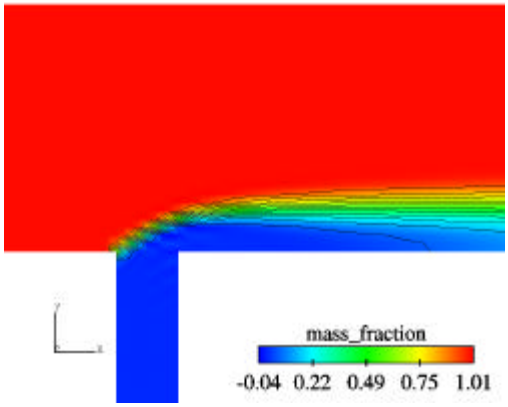

Figure 4: Result for $Pe^m_K = 10^1$, stable

For $Pe^m_K \approx 10^2$, instabilities start to appear when Galerkin approximation is employed. Figure 5 shows the comparing between results for the solutions in the range $10^2 \leq Pe^m_K \leq 10^4$.

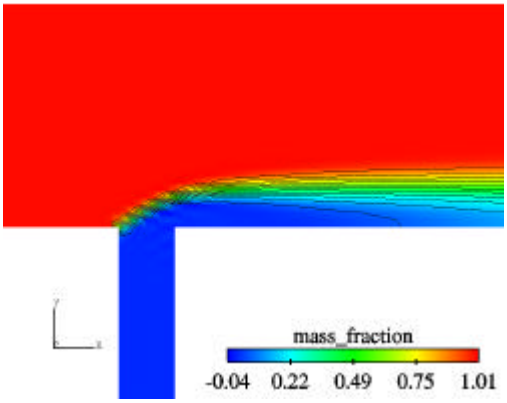

(a) $Pe^m_K \approx 10^2$, Galerkin approximation

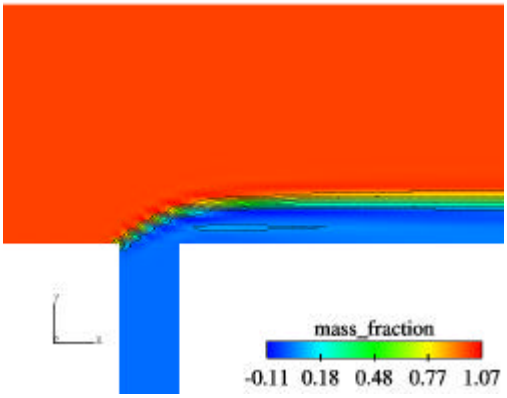

(b)$Pe^m_K \approx 10^2$, SUPG approximation

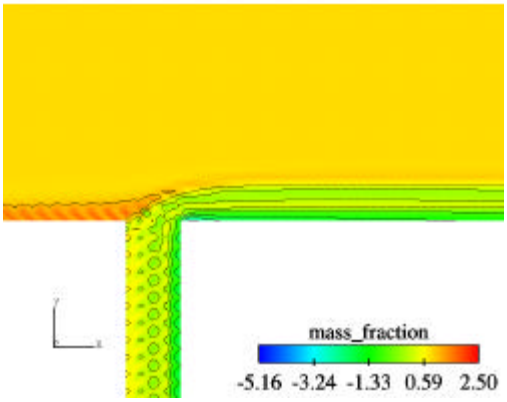

(c) $Pe^m_K \approx 10^3$, Galerkin approximation

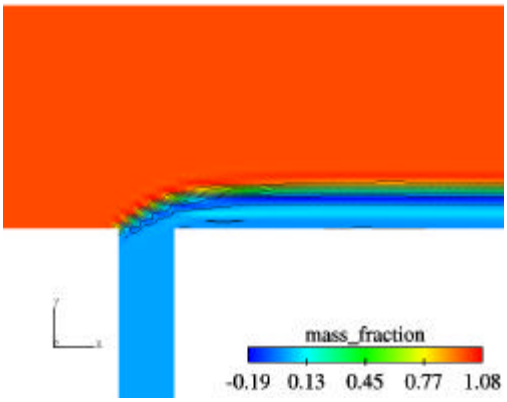

(d) $Pe^m_K \approx 10^3$, SUPG approximation

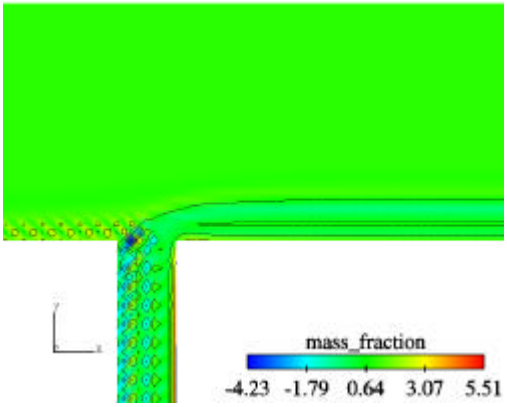

(e) $Pe^m_K \approx 10^4$, Galerkin approximation

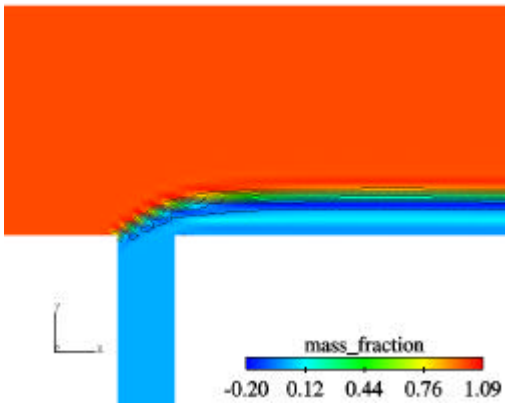

(f) $Pe^m_K \approx 10^4$, SUPG approximation

Figures 5: Solutions for the Galerkin (a, c and e) and SUPG (b, d and f) schemes

It is observed that the instabilities are created forming a “crocodile pattern”, and that the instabilities get much more smooth when the SUPG scheme is used.

Within the stabilized results, the mass fraction profile in the *y* direction was analyzed in a position 3x*D* (*D* = larger tube diameter) from the injection (Fig. (6)). In results for $Pe^m_K \approx 10^3$ and $Pe^m_K \approx 10^4$, light numerical instabilities exist giving values lower than zero and higher than one. The region where most of the mixture occurs is in the range $0.11 \leq y/D \leq 0.26$.

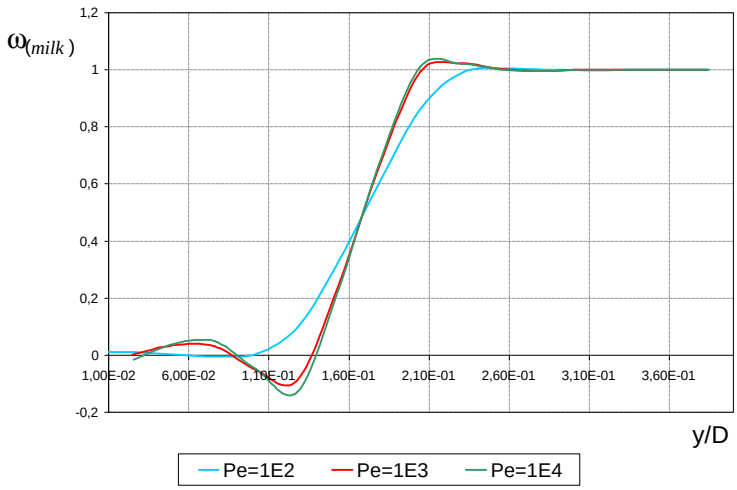

Figure 6: Mass fraction profile for the skimmilk, 3x*D* from injection

4.2. 3D simulations

In this section, 3D results of mass fraction and velocity field are presented. Four different geometries were employed with the dimensions based in industrial tubes for milk processing, where the diameter of the cream pipe varies from ¼ inch up to 1 inch, as shown in Fig. (7). Each model has 13056 hexaedric elements. The tubes are rigid and the species were considered as newtonian incompressible fluids.

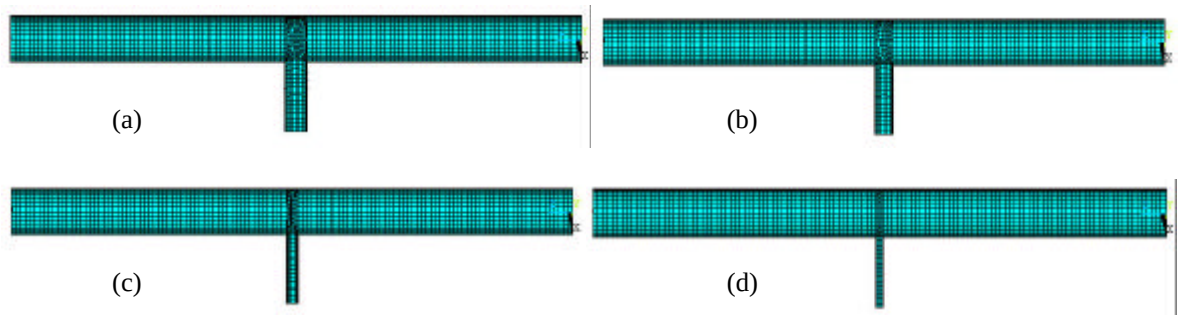

Figure 7: 3D mesh for simulations: diameter of cream pipe with (a) 1 inch (0.0254 m), (b) ¾ inch (0.01905 m), (c) ½ inch (0.0127 m) and (d) ¼ inch (0.00635 m).

The prescribed milk inlet velocity is calculated in order to obtain a Reynolds number inside the laminar range and a mixture with 92,5% of simmilk and 7,5% of cream in the outlet.

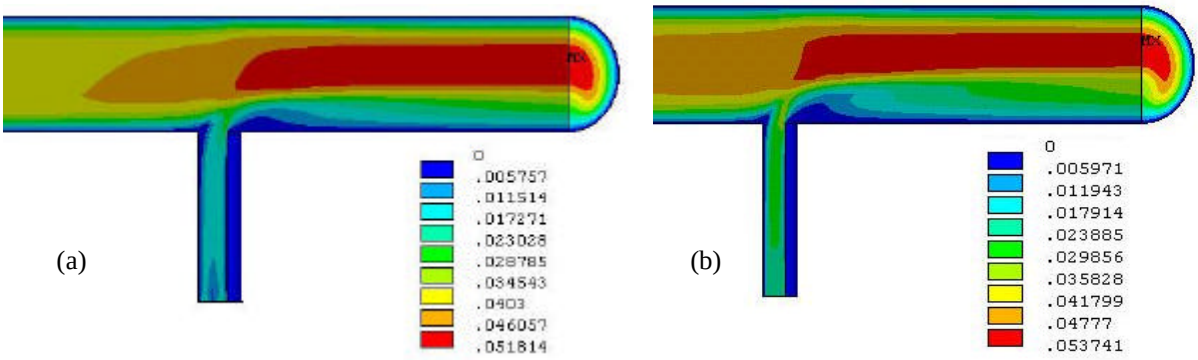

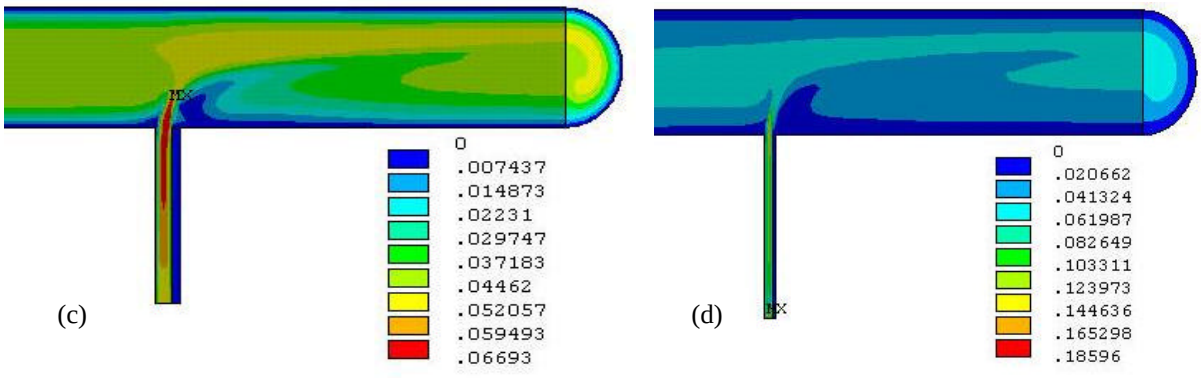

Figure 8: Velocity fields: diameter of cream pipe with (a) 1 inch, (b) ¾ inch, (c) ½ inch and (d) ¼ inch

In Fig. (8), one may see that the cream flux behaves like a restriction to the skimmilk flow, deviating its flow for the upper pipe section. This effect decreases when the cream tube diameter is reduced. The pressure fields are depicted in Fig. (9).

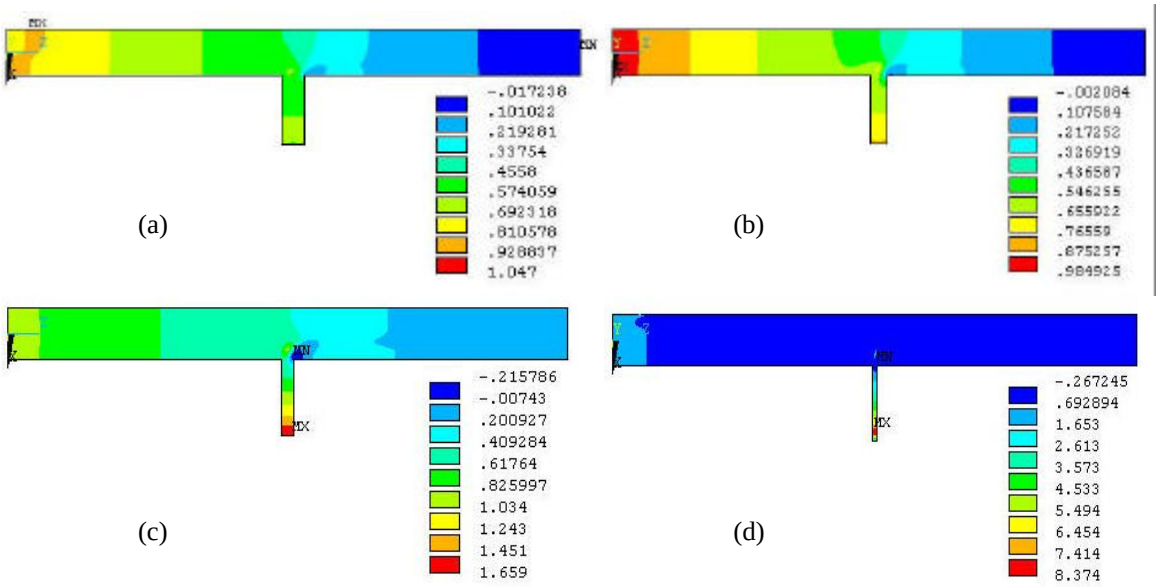

Figure 9: Pressure fields: diameter of cream pipe with (a) 1 inch, (b) ¾ inch, (c) ½ inch and (d) ¼ inch

As expected, it is possible to see that the pressure drop along the cream pipe increases with the diameter, demanding more pumping power. This is due to the larger friction area and also to the need of higher velocities in order to maintain the same mass flux. In this way, the power requirement becomes a relevant parameter for project design.

Figure (5) shows the mass transfer process for each case, in a pipe longitudinal section. Figure (6) shows this process in the pipe cross section.

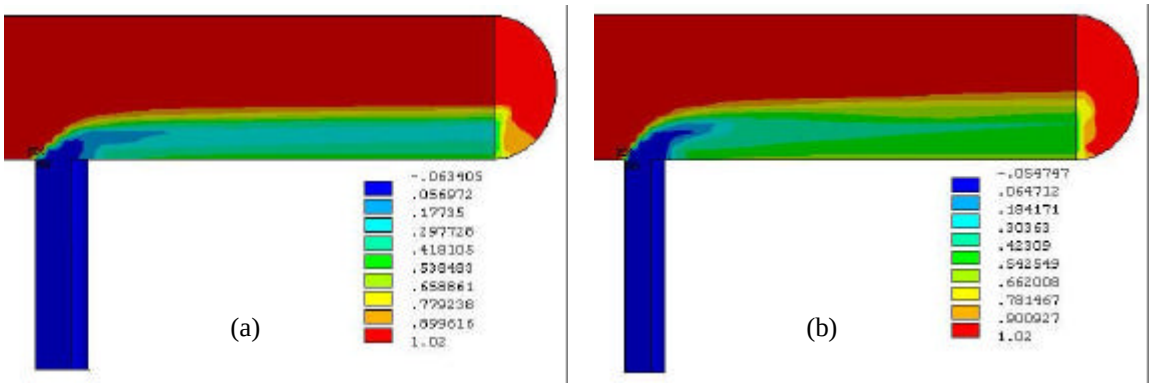

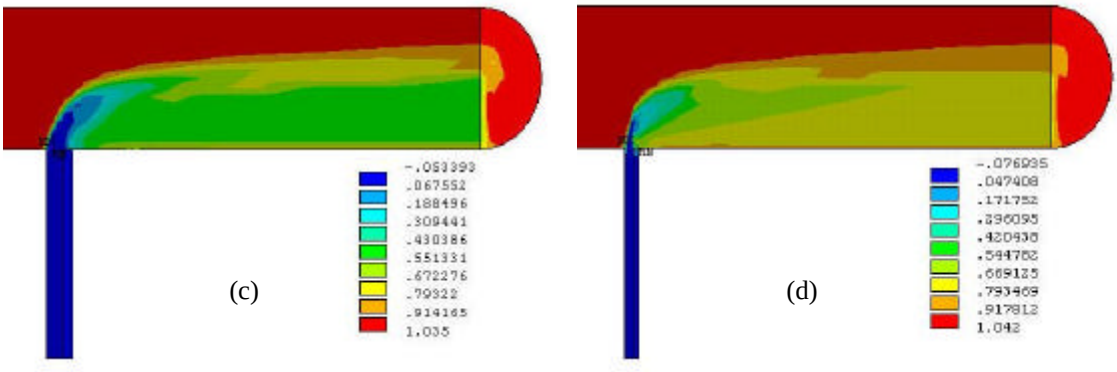

Figure 10: Smimilk mass fraction: diameter of cream pipe with (a) 1 inch, (b) ¾ inch, (c) ½ inch and (d) ¼ inch

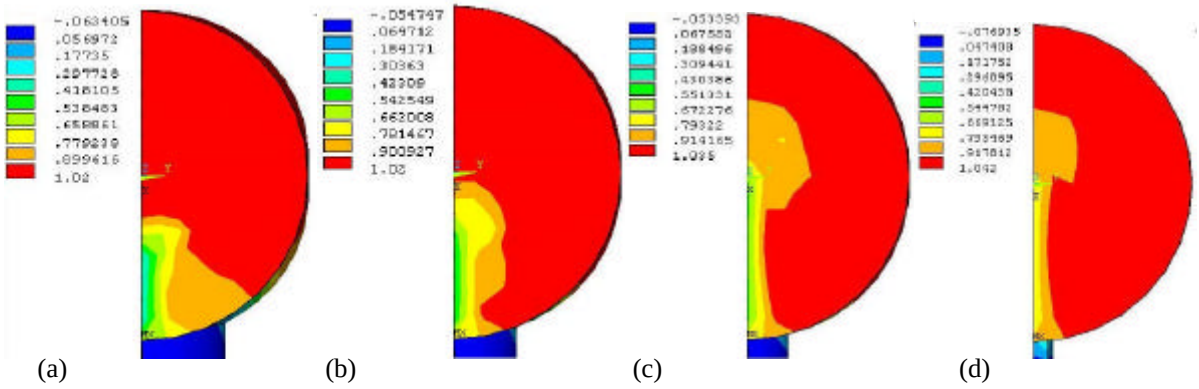

Figure 11: Skimmilk mass fraction (at the outlet): diameter of cream pipe with (a) 1 inch, (b) ¾ inch, (c) ½ inch and (d) ¼ inch

It was expected that with higher cream speed through the thinner cream pipe, the mixture at the outlet would be more homogeneous, increasing the convection importance in the advective-diffusive process. Although, the cross section of the outlet in Figure (11) shows that the mixture homogenization did not occur in the direction of the sides of the pipe, the mixture was deviated to the superior pipe region. The results do not show effectiveness of the cream-skimmilk homogenization.

5. Conclusions

In this paper, some aspects of the mechanical modeling of cream injection in skimmilk were explored. The problem was modeled as a multicomponent system with constant properties, according to continuum mechanics theory.

Using a finite element model, the velocity field of a laminar flow was calculated for a 2D domain, and it was used to calculate the mass fraction field. As the Peclet number became too high for realistic diffusion coefficients, it was necessary to use a stabilized formulation. The stabilized SUPG simulations were compared to simulations using classic Galerkin approximations for a Peclet range from 10^2 to 10^4. The results using SUPG showed stabilization characteristics not found in non-stabilized simulations.

To observe more realistic results, a 3D mesh was employed. The results for different geometries were observed. The effectiveness of mixture and pressure drop were compared as important parameters for equipment project and design.

6. Acknowledgements

The authors F. S. Franceschini and S. Frey gratefully acknowledge the financial support provided by the agency CNPq through grants n^o 133608/01-8 and 350747/93-8, respectively, and D. H. Girotti-Fontana thanks for the undergraduate scholarship provided by PIBIC/CNPq-UFRGS.

7. References

Brasil Junior et al. “Métodos de Estabilização” In: Projeto FAP-DF no 191.000.285/94 – Relatório Técnico Final, Agosto 1997.

Brooks, A.N., Hughes, T.J.R. , 1982 “Streamline Upwind/Petrov-Galerkin formulations for convective dominated flows with particular emphasis on the incompressible Navier-Stokes equations”, *Comput. Methods Appl. Mech. Engrg.*

Vol. 32, pp. 199-259.

Franca, L. P., Frey, S. e Hughes, T.J.R., 1992, “Stabilized finite element methods: I. Application to the advective-diffusive model”, Comput. Methods Appl. Mech. Engrg., Vol. 95, pp. 253-276.

Franca, L.P. and Frey, S., 1992, “Stabilized finite element methods: II. The incompressible Navier-Stokes equations”, Comput. Methods Appl. Mech. Engrg., Vol. 99, pp. 209-233.

Gurtin, M. E. “An introduction to continuum mechanics”, Academic Press, U.S.A., 1981.

Hughes, T. J. R.; Franca, L. P.; Hulbert, G. M.; Johan, Z. & Shakib, F., “The Galerkin/Least-squares method for advective-diffusive equations”. In: Recent developments in computational fluid dynamics. New York, U.S.A., 1988.

Kumar, A., Swartzel, K. R., “Selected food engineering problems and their solution through FEM”. In: Advances in Finite Element Analysis in Fluid Dynamics, ASME, vol. 171, 107 – 113, 1993.

Panton, R. L., “Incompressible Flow”, John Wiley & Sons, U.S.A.

Slattery, J. C., 1999, “Advanced Transport Phenomena”, Cambridge University Press, U.S.A.

Tetra Pak Processing Systems Ab., “Dairy Processing Handbook”. Sweden: Teknotext AB. 1995.

Truesdell, C. and Noll, W., 1965, “The non-linear field theories of mechanics”, In. *S.* Flugge, Handbuch der Physik, Vol. 3/3, Berlin: Springer-Verlag.

Truesdell, C. and Toupin, R. A., 1960, “The classical field theories”, In: S. Flugge, Handbuch der Physik, Vol. 3/1, Berlin: Springer-Verlag.

Xia, B., Sun, D., “Applications of computational fluid dynamics (CFD) in the food industry: a review”. In: Computers and Electronic in Agriculture, in press, 2002.